FILE COPY

ESD-TR-74-138

ESD ACCESSION LIST
DRI Call No. 80789
Copy No. 1 of 2 cys.

# Technical Report 501

I. Kupiec

# Compensation of Multipath Angular Tracking Errors in Radar

20 March 1974

Prepared for the Office of the Chief of Research and Development,
Department of the Army,
under Electronic Systems Division Contract F19628-73-C-0002 by

**Lincoln Laboratory**

MASSACHUSETTS INSTITUTE OF TECHNOLOGY

LEXINGTON, MASSACHUSETTS

AD0781100

Approved for public release; distribution unlimited.

MASSACHUSETTS INSTITUTE OF TECHNOLOGY
LINCOLN LABORATORY

# COMPENSATION OF MULTIPATH ANGULAR TRACKING ERRORS IN RADAR

*I. KUPIEC*

*Group 34*

TECHNICAL REPORT 501

20 MARCH 1974

Approved for public release; distribution unlimited.

LEXINGTON MASSACHUSETTS

The work reported in this document was performed at Lincoln Laboratory, a center for research operated by Massachusetts Institute of Technology. The work is sponsored by the Office of the Chief of Research and Development, Department of the Army; it is supported by the Advanced Ballistic Missile Defense Agency under Air Force Contract F19628-73-C-0002.

This report may be reproduced to satisfy needs of U.S. Government agencies.

Non-Lincoln Recipients

**PLEASE DO NOT RETURN**

Permission is given to destroy this document when it is no longer needed.

ABSTRACT

Multipath compensation techniques for radar applications are being evaluated. Three methods which comprise an extension of the conventional monopulse and a fourth that utilizes coherent samples taken across the antenna aperture were considered. The performance in the presence of a single specular reflection from the ground is compared by means of Monte Carlo computer simulations. The aperture sampling technique using a minimizing search processing is found to outperform the other methods.

Accepted for the Air Force
Eugene C. Raabe, Lt. Col., USAF
Chief, ESD Lincoln Laboratory Project Office

CONTENTS


| | | |
|---|---|---|
| | Abstract | iii |
| | INTRODUCTION | 1 |
| I. | STATEMENT OF THE PROBLEM | 1 |
| II. | COMPLEX MONOPULSE | 5 |
| | A. Complex Monopulse with Terrain Calibration | 5 |
| | B. Frequency Diversity | 7 |
| | C. Boresight Diversity | 13 |
| III. | APERTURE SAMPLING | 16 |
| | A. Principle and Limitations | 17 |
| | B. Two Practical Methods | 18 |
| | C. Simulation Results | 20 |
| | D. Multiple-Specular and Diffuse Ground Reflections | 23 |
| IV. | CONCLUSIONS | 27 |
| | References | 29 |

# COMPENSATION OF MULTIPATH ANGULAR TRACKING ERRORS IN RADAR

## INTRODUCTION

This report summarizes a study of multipath, i.e., ground reflection, compensation techniques, which was conducted at Lincoln Laboratory recently. It addresses the problem of elevation angle measurement in the presence of multipath interference. The study was motivated by a consideration of a specific network of ground-based radars; however, the results and recommendations apply equally well to other radar systems.

In what follows, the basic multipath problem is formulated and described. It is also presented as an angular resolution problem. Subsequently, compensation techniques are described and evaluated by means of Monte Carlo simulations. Three of the techniques comprise extension of the conventional monopulse, referred to here as Complex Monopulse schemes. The fourth technique, the Aperture Sampling method, involves processing of coherent samples taken across the radar's antenna aperture.

## 1. STATEMENT OF THE PROBLEM

A radar system tracking a target at low elevation angles, namely, within one or two beamwidths above the horizon, experiences serious difficulties. These difficulties result from the presence of a strong ground reflection or multipath signal. The elevation angle is the most strongly affected tracking parameter. In a conventional closed-loop monopulse tracker, tracking becomes erratic and in certain cases may be completely lost. In an open-loop tracker, such as would be used with a phased-array radar, accurate estimation of the elevation angle becomes difficult because of the presence of a large varying systematic (bias) error. In both cases the precision of such an estimation degrades at elevation angles in which destructive interference due to multipath reduces the signal-to-noise ratio.†

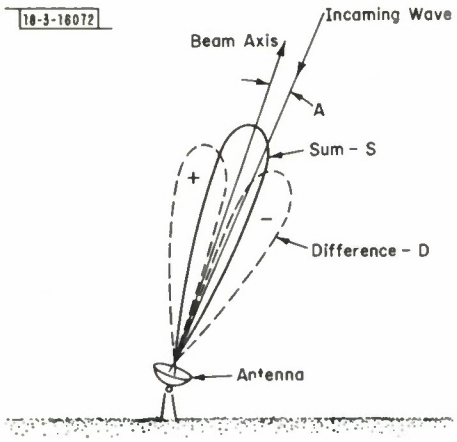


Fig. 1. Amplitude monopulse.

The problem can be best understood by considering the operation of the monopulse technique. It is assumed that the radar measures elevation angle by using an amplitude monopulse. The target elevation angle off the antenna axis is denoted A, and the sum and difference patterns are denoted S and D, respectively (see Fig. 1). The signals received in the sum and difference

† The precision is proportional to the inverse of the square root of signal-to-noise ratio.

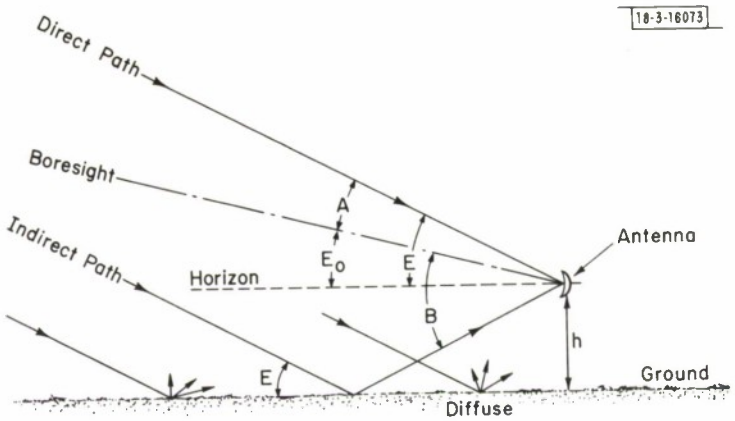


Fig. 2. Multipath geometry.

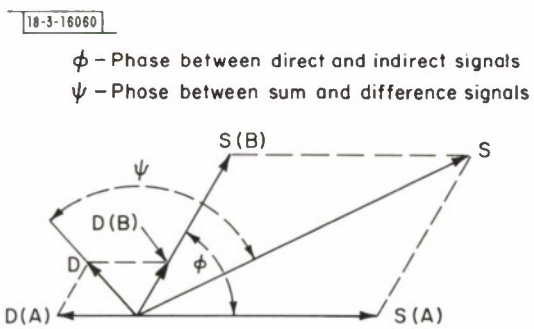


Fig. 3. Sum and difference signals phasor diagram in the presence of multipath.

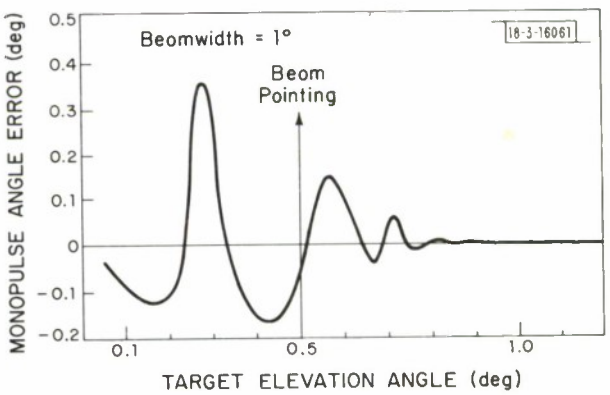


Fig. 4. Multipath bias error of conventional monopulse.

channels are then kS(A) and kD(A). Here k is a proportionality factor that accounts for all the terms that enter the radar range equation. The off-axis angle is obtained from the normalized error signal, D/S. That is, within the sum beamwidth this ratio is proportional to the off-axis angle

$$A = \frac{1}{p} \frac{D(A)}{S(A)} \quad , \tag{1}$$

where 1/p is a proportionality constant. The sense of the angle with respect to the beam axis is related to the phase angle between D(A) and S(A). In free space, ideally, D(A) and S(A) are either in-phase or out-of-phase depending on the sign of A. The target elevation angle is obtained by combining the estimated A with the known beam axis pointing angle. In normal closed-loop angle tracking A is small compared to beamwidth.

In the presence of multipath, i.e., reflection from the ground, the situation is quite different. The relation between the off-axis angle and the normalized error signal is not as simple, and the phase between the sum signal and difference signal can take any value. Referring to Fig. 2, one can easily show that in the presence of multipath the signals received by the sum and difference channels are given by

$$D = S(A) + \Gamma \exp(i\varphi_d)\, D(B) \tag{2a}$$

$$S = S(A) + \Gamma \exp(i\varphi_d)\, S(B) \quad . \tag{2b}$$

Here $\Gamma$ is the complex ground reflection coefficient, and $\varphi_d$ is the phase retardation due to the longer pathlength of the indirect signal. B is the angle-of-arrival of the indirect return with respect to the beam axis. The total phase difference between the direct and indirect signals is given by

$$\varphi = \varphi_\Gamma - \frac{4\pi h}{\lambda} \sin E \quad , \tag{3}$$

where $\varphi_\Gamma$ is the phase of the reflection coefficient, $\lambda$ is the wavelength, h is the antenna's phase-center height above ground, and E is the target's elevation angle. Equations (2a) and (2b) are displayed in a form of a phasor diagram in Fig. 3. It is seen that since $\varphi$ varies with elevation angle, so will $\psi$, the phase between the sum and difference signals. The phase can be anywhere between 0° and 360° and not just 0° or 180°. The usual monopulse radar is designed to determine the real part of D/pS and to report this quantity as the value of A = D(A)/pS(A). When the multipath contribution is large, D/pS is drastically different from D(A)/pS(A), yielding a large error in a conventional monopulse. Such a condition occurs at low elevation angles when the multipath signal arrives through the main beam.

Figure 4 shows a typical multipath error; the quasi-periodic behavior stems from the fact that $\varphi$ can vary many multiples of $2\pi$ for moderate variations in E. The information presented in Fig. 4 was obtained by fixing the beam axis pointing angle and varying the target elevation (letting the target coast through the beam). This depicts the error in an open-loop tracker. In a closed-loop tracker the curve describes the erroneous pointing angle of the tracking antenna. It is observed that the error decreases as the elevation angle increases. This is caused by the fact that for the larger elevation angles the multipath contribution is received through sidelobes. When the multipath enters the receiver through sidelobes, the error is smaller by a few orders of magnitude (depending on the sidelobe level). It can then be handled separately and will not

require the amount of sophistication needed for the more serious case when both, direct and indirect returns, are received by the main beam. Since the elevation angle in most applications varies with time, the multipath error is a time-dependent bias error. It is worthwhile to note at this point that the model used here assumes a flat earth and a target at infinity. It implies the existence of only one distinct specular reflection and that the target return is a plane wave. The reflection coefficient was assumed to be $-1.0$. Such a model will be used in describing the compensation schemes. The effect of multiple specular reflection as well as diffuse reflection and curved earth effect will be discussed later.

It is seen then that in the presence of multipath, at low elevation angles, a conventional monopulse tracking system has a large varying bias error. In addition, since at certain elevation angles the interfering multipath signal may be out-of-phase with respect to the direct signal, the signal-to-noise ratio is substantially smaller yielding a larger angular random error. Thus, any scheme which tries to alleviate the difficulties experienced by a tracking radar at low elevation angles should strive to achieve the following:

(a) Eliminate the large multipath bias,

(b) Obtain an angular rms error of the same magnitude as can be obtained by the system when it operates in free space.

More insight can be gained by viewing the problem in a different manner. Using a flat surface model, the multipath can be viewed as coming from the image of the target. If the surface is curved or rough the image is diffused, and the multipath contribution is modified in strength. However, for a very low elevation angle this represents a small modification. In this case the target and its image occupy the same range cell and their angular separation is less than a beamwidth. (The range difference between the target and its image, at low elevation angles, is usually much smaller than the range resolution capability of the radar. Very large bandwidths would be required to resolve the target from its image in range.) In order to measure the elevation angle, one has to resolve the target from its image in elevation angle and then estimate its elevation. In essence this amounts to nulling the multipath contribution while the target parameters are estimated. It is done by appropriate data processing and does not have to be realized in the antenna pattern. In the absence of any a priori information concerning the number of plane waves arriving at the radar, the angular resolution capability of the antenna is about one beamwidth, hence this technique seems impossible. If, however, the number of incoming plane waves is known, the angular resolving power is less than a beamwidth and is limited only by the presence of noise. Since in the presence of multipath one is usually able to guess the number of incoming waves it should be possible to resolve the target from its image. Most of the schemes to be described in this report assume one multipath component. In such a case the presence of more than one multipath contribution produces errors.

In discussing the various multipath compensation techniques the problem of illuminating the target in the presence of multipath will be disregarded. This difficulty arises in radar applications when the direct and indirect signals may arrive at the target out-of-phase. In practice, perfect cancellation of signal does not occur, rather large reduction of signal level is experienced. Thus, in subsequent sections, it will be assumed that the reflected signal is strong enough to be detected by the radar. Such a problem does not exist in beacon tracking.

## II. COMPLEX MONOPULSE

### A. Complex Monopulse with Terrain Calibration

As was noted in the previous section, the normalized error signal in the presence of multipath is a phasor whose phase and amplitude depend on the multipath signal. Using coherent detection, the amplitude and phase of the normalized error signal can be determined and serve as two independent sources of information for angle estimation. This use of the information contained in the quadrature (as well as the real) component of the normalized error signal to facilitate the determination of the true elevation angle in the presence of multipath was proposed by Sherman.[1] He named this approach the Complex Indicated Angle to emphasize that the complex normalized error signal is interpreted as a complex angle. In this report, schemes that utilize the quadrature component of the difference channel are called Complex Monopulse.

The normalized difference channel signal in the presence of one multipath component is given by

$$\frac{D}{S} = \frac{D(A) + re^{i\varphi}D(B)}{S(A) + re^{i\varphi}S(B)} = \frac{\frac{D(A)}{S(A)} + re^{i\varphi}\frac{D(B)}{S(B)}\frac{S(B)}{S(A)}}{1 + re^{i\varphi}\frac{S(B)}{S(A)}} = \frac{p(A + rge^{i\varphi}B)}{1 + rge^{i\varphi}} \tag{4}$$

where $r$ is the magnitude of the reflection coefficient, $\varphi$ is the total phase difference between the direct and indirect paths, and $g$ is the sum voltage pattern ratio $S(B)/S(A)$. The complex indicated angle is

$$\frac{1}{p}\frac{D}{S} = x + iy = \frac{A + gre^{i\varphi}B}{1 + gre^{i\varphi}} \quad . \tag{5}$$

From a single pulse return one may retrieve two independent quantities, $x$ and $y$. The number of unknowns on the right-hand side of Eq. (5) is five, namely, $A$, $B$, $g$, $r$, $\varphi$. However, when the multipath is due to a flat ground plane with zero slope, $A$ and $B$ are related in the following manner.

$$A = E - E_o \quad , \tag{6a}$$

$$B = -E - E_o \quad , \tag{6b}$$

where $E$ is the true target elevation and $E_o$ is the beam-axis elevation. If the slope is not zero but known, it could be incorporated in Eq. (6b). In addition, $\varphi$ is related to $E$ via Eq. (3). Thus if one knows the reflection coefficient there is enough information in one pulse to eliminate the multipath and solve for the true elevation angle. In practice, one may choose to develop an analytical algorithm to solve a set of four equations or use a graphical display. Originally, Sherman proposed using a graphical display. It is worthwhile to describe this method since it highlights the inherent difficulties of this version of Complex Monopulse. It can be shown that when the beam-axis angle is fixed the complex indicated angle [Eq. (5)] describes a spiral in the complex plane as the target coasts through the beam (Fig. 5). This can be seen intuitively by noting that Eq. (5) describes a circle in the complex plane when $\varphi$ varies and the rest of the parameters in Eq. (5) remain constant. When the elevation angle varies and the beam axis is fixed, $A$ and $B$ as well as $\varphi$ vary. For a small variation in elevation angle the locus of points approximates a small circular arc. For large variation of the elevation angle, the locus is a collection of small circular arcs with variable curvature; this yields a spiral shape. Such a spiral with the true elevation angle as a parameter along the curve is shown in Fig. 5.

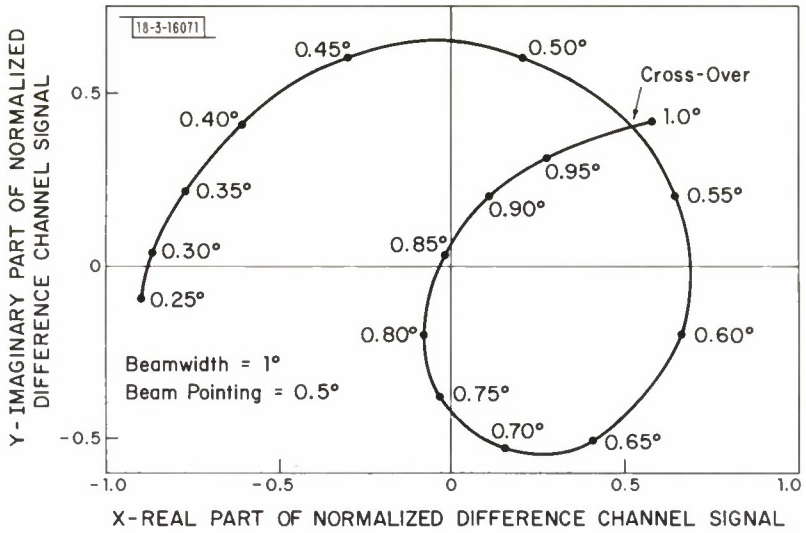


Fig. 5. Computed spiral with target elevation as a parameter.

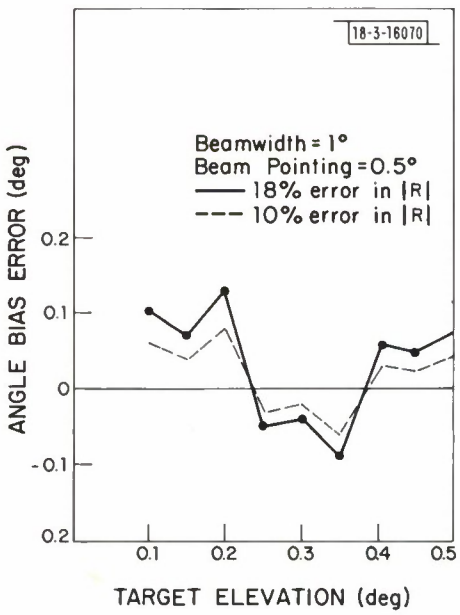


Fig. 6. Errors due to uncertainty in value of the magnitude of the reflection coefficient, $|R|$.

A practical implementation consists of displaying a measured spiral (calibration spiral) on a CRT. The elevation angle of a target is then determined from the location of a measured point on the display. However, there is an ambiguity where the spiral crosses itself. When the antenna center is high, there may be many crossing points. In the absence of noise or jitter the measured points fall on the calibration spiral and only the crossing points are ambiguous. But in the actual radar, errors are present, and the measured point will not lie precisely on the spiral. In such a case, an estimate is obtained by projecting to the nearest point on the calibration spiral. If the measured point is in the vicinity of a crossing point, the ambiguity causes large error.

Other difficulties stem from the need to know the ground reflection coefficient. If a display is used, equivalently, calibration spirals corresponding to different values of reflection coefficients are needed. The characteristics of the ground surface around the radar change with time. Such changes are due to moisture variations as a result of rainstorms or snowfall. They may also be caused by slow variation due to natural growth of the vegetation in the vicinity of the radar. These variations introduce uncertainty as to which value of reflection coefficient or which calibration spiral should be used. If errors of the order of 10 to 20 percent in estimating the reflection coefficient occur, the observed variations in bias errors are excessive. Figure 6 shows the residual elevation bias for such errors in reflection coefficient whose nominal value is $-1$. As the uncertainty in value of the reflection coefficient increases, the curves tend to resemble the error curve (see Fig. 4) with no multipath compensation. The simulation results presented in Fig. 6 were derived by using an analytical algorithm. Two cases corresponding to 10- and 18-percent errors in estimating the magnitude of the ground reflection coefficient are shown. These results apply also to a case where a displayed spiral is used and correspond to a situation where the calibration spiral was not changed to agree with surface condition variations.

In a field radar system, the displayed spirals are obtained by measurements and are stored in the radar. This procedure, in principle, enables one to overcome problems that arise due to irregularities of the terrain. This will require measurements for a number of azimuth directions and possibly for many ground conditions. Storage of such a large amount of information and the need to be able to change the display as the target moves or as the ground conditions change soon becomes a substantial load on the radar's computer resources, rendering such an approach impractical. In the presence of multiple specular reflections, small loops are superimposed on the spirals. These add ambiguities and result in additional sources of error.

In view of the difficulties delineated above, it is believed that this approach is not a reliable solution that could be implemented in a field radar for the multipath problem.

### B. Frequency Diversity

It was shown previously that a return from a single pulse in the presence of multipath contains two independent pieces of information, provided the radar is instrumented to measure the quadrature component of the normalized error signal. In view of the fact that the number of unknowns is greater than two, the return from a single pulse is not sufficient for a unique determination of the true elevation angle. In order to recover the true elevation angle from a single return, one needs additional information including the magnitude and phase of the reflection coefficient. To circumvent difficulties arising from uncertainties in assuming the value of the reflection coefficient, a scheme that effectively measures the reflection coefficient in real time is needed. This could be achieved by combining the information from two or three pulse returns. Such a scheme will now be described in detail.

The target is assumed to be within one beamwidth above the horizon so that the direct and reflected returns are received through main beam. A long range to the target and flat ground are also assumed. This implies that in the vicinity of the antenna and the reflecting area the echo is a plane wave and that there exists only one specular reflection. Under the above assumptions the normalized error signal can be expressed in the form

$$\frac{1}{p}\frac{D}{S} = x_1 + iy_1 = \frac{A + gre^{i\varphi_1}B}{1 + gre^{i\varphi_1}} \quad , \tag{7}$$

where the notation of the previous section is used. The subscript 1 indicates a return from the first pulse. The product gr may be considered as one variable, u. Thus there are four unknowns, A, B, u, and $\varphi_1$. The phase shift, $\varphi_1$, between the direct and indirect rays depends on a few parameters [Eq. (3)], one of which is the frequency. It can be changed by changing the frequency. Explicitly the phase change is given by

$$\Delta\varphi_1 = -\frac{4\pi h}{c}\,\Delta f \sin E \quad , \tag{8}$$

where $\Delta f$ and c are the frequency increment and speed of light, respectively. Therefore, subsequent transmission of a second pulse at a different frequency can provide an independent measurement:

$$x_2 + iy_2 = \frac{A + gre^{i\varphi_2}B}{1 + gre^{i\varphi_2}} \quad . \tag{9}$$

It is assumed that in the short time that elapses between the pulses, the elevation angle changes a negligible amount. Also, frequency jumps of less than 20 percent are contemplated, in which case changes in g and r are negligible. Since $\varphi_2$ is unknown there are now five unknowns, but use of specific relation between A and B for the case of specular reflection [Eq. (6a, b)] provides an additional equation to enable a unique solution. In summary, the proposed scheme consists of combining the information obtained from pairs of pulses each centered at a different frequency. All the parameters but the phase are assumed to remain constant. The equations relating the various parameters are given by:

$$x_1 + iy_1 = \frac{A + ue^{i\varphi_1}B}{1 + ue^{i\varphi_1}} \quad , \tag{10a}$$

$$x_2 + iy_2 = \frac{A + ue^{i\varphi_2}B}{1 + ue^{i\varphi_2}} \quad , \tag{10b}$$

$$A = E - E_o \quad , \tag{10c}$$

$$B = -E - E_o \quad . \tag{10d}$$

Four equations relating the five unknowns are obtained from (10a, b). A fifth equation is obtained by combining (10c) and (10d).

The equations can be solved in a simple manner if one realizes that as long as A, B, and u remain constant the locus of the points $(x_i, y_i)$ in the complex plane is a circle whose center is on the real axis (Fig. 7). Thus, given two points on the circle one can determine its center and

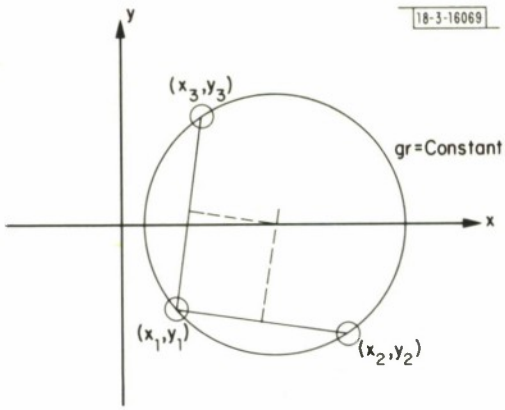


Fig. 7. Geometrical interpretation of the frequency diversity algorithm.

radius. That is, if the center is at (C, 0) and the radius is R, they are related to the measured points by:

$$C = \frac{x_2^2 - x_1^2 + y_2^2 - y_1^2}{2(x_2 - x_1)} \quad , \tag{11a}$$

$$R = [(x_1 - C)^2 + y_1^2]^{1/2} \quad . \tag{11b}$$

The points at which the circle intercepts the real axis are characterized by $y_i = 0$ and correspond to $\varphi = 0°, 180°$. The x coordinates of these points are

$$x_0 = \frac{A + uB}{1 + u} \quad , \tag{12a}$$

$$x_{180} = \frac{A - uB}{1 - u} \quad . \tag{12b}$$

The circle's center is half way between these points hence,

$$C = \frac{A - u^2 B}{1 - u^2} \quad , \tag{13a}$$

$$R = \frac{u(A - B)}{1 - u^2} \quad . \tag{13b}$$

A and B can now be expressed in terms of C, R, and u:

$$A = E - E_o = C - uR \tag{14a}$$

$$B = -E - E_o = C - \frac{R}{u} \quad . \tag{14b}$$

Eliminating A and B yields

$$Ru^2 - 2(C + E_o)\, u + R = 0 \quad . \tag{15}$$

Since $E_o$ is known, and C and R have been determined from measurements, u can be determined. Subtracting Eq. (14b) from Eq. (14a) yields

$$E = \frac{R}{2}\left(\frac{1}{u} - u\right) \quad . \tag{16}$$

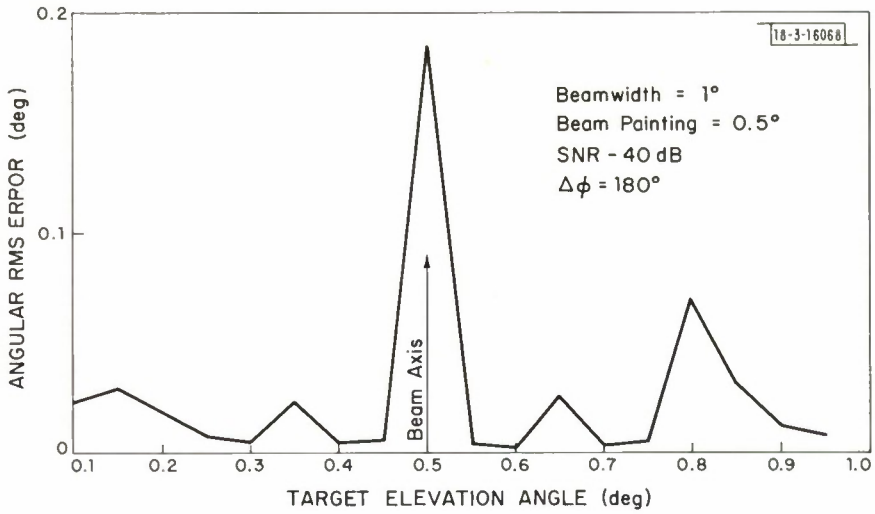


Fig. 8. Angular rms error, frequency diversity.

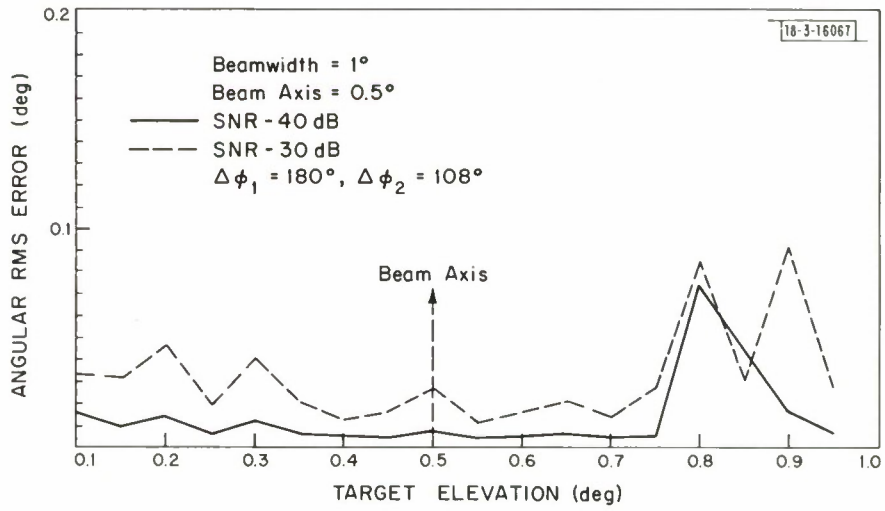


Fig. 9. Angular rms error, frequency diversity.

Equation (16) yields E, the true elevation angle. E and $E_o$ determine A and B; combining this information with the antenna pattern will yield g, which in turn yields r. $\varphi_\Gamma$ can be determined by solving for $\varphi_2$ or $\varphi_1$ and using Eq. (3). This shows that indeed the reflection coefficient is measured in real time. Of course, the radar is interested only in E, thus only the algorithm that determines E would be incorporated in a practical system.

Until now it was assumed that $(x_1, y_1)$ and $(x_2, y_2)$ are known exactly, disregarding the fact that the measurements are corrupted by noise. The presence of noise is shown in Fig. 7 by the small circles around the nominal points. The radius of these circles represents the standard deviation of the measurement errors. The geometrical interpretation of the algorithm given above is also depicted in Fig. 7. The first step was to determine the center of the circle given two points on the circle. The center is the intersection of the perpendicular bisector of the chord and the real axis. In the presence of measurement error the ends of the chord may lie anywhere on the plane. Most of the time they lie inside the small circles. The effect of the noise is to yield an erroneous location of the center which in turn produces an error in the estimated elevation angle. It is intuitively clear that this error will be large if the chord length is of the same order of magnitude as the standard deviation of the noise. Thus to effect a reliable measurement, $\Delta\varphi = \varphi_1 - \varphi_2$ must be made large enough to yield a large chord. The optimum value is not known a priori in any specific case since it depends on the value of u. On the other hand, a large change in phase may yield a situation depicted by the pair $(x_1, y_1)$ and $(x_3, y_3)$. In this case the chord is almost perpendicular to the real axis. The bisector intersects the real axis at a very small angle. Small measurement errors can cause very large errors in locating the circle's center. If the chord happened to be perpendicular to the real axis and there are no errors, the solution becomes indeterminate. To overcome this problem one may use three pulses. In such a case one has the option of peaking the pair of points that lies on the same side of the real axis or determining the center by triangulation. Both solutions yield similar results.

The frequency-diversity method was evaluated by simulation. Figure 8 shows a case where two pulses were used. The peak error at the center is related to the difficulty described above, i.e., when the two points define a chord that is almost perpendicular to the real axis. Figure 9 describes errors for the same case when three pulses were used. The peak at the center was eliminated. It is seen that within a quarter of a beam on each side of the beam axis the system performs just like a monopulse in free space, with a rms angle error of the order of $BW/k\sqrt{SNR}$ (Ref. 2). Here, BW is the beamwidth, and k is a normalized error slope, and SNR is the signal-to-noise ratio. Figure 10 depicts the bias error which is the error of the mean estimate. Comparison of Figs. 10 and 4 shows that the measurement is, for all practical applications, biasless. Such measurements will enable a recursive tracking algorithm to perform at low elevation angles as well as at high elevation angles.

For the sake of clarity (and expediency) only a simplified analysis was pursued thus far. This was done with full awareness of the various approximations used and at least some of their implications. In order to complete the description of the scheme, the limitations resulting from such approximations are listed below. (Some obvious extensions needed to overcome the restrictions are also described.)

It was assumed that the direct and indirect returns enter the antenna through the main beam, so that the linear relation between the normalized error voltage and the off-axis angle could be used. In principle the analysis could be extended to include cases where the multipath enters

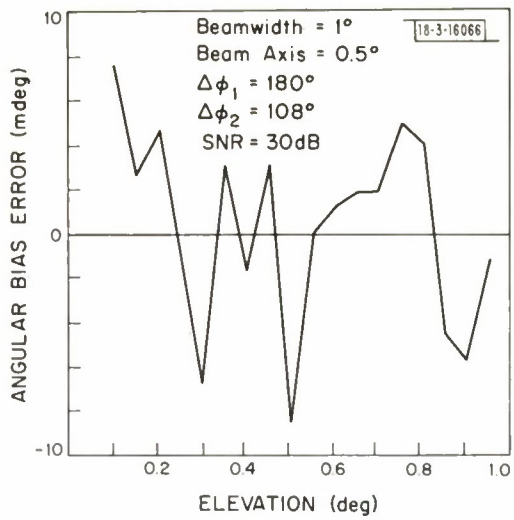


Fig. 10. Angular bias error, frequency diversity.

through a sidelobe while the direct return is within the beam. This would require the knowledge of the nonlinear (and probably multivalued) relation between the error voltage and the off-axis angle pertaining to large angular offsets. Such an extension is very complicated and is not considered to be practical. Furthermore, in these cases the method is sensitive to random noise-like errors. This sensitivity stems from the fact that, for sidelobe multipath interference, gr is small, and the circle in the complex plane is small. Since the noise level does not change, it is difficult to maintain a large chord length to rms noise ratio (see Fig. 7). Therefore, the method is not useful for reduction of multipath error due to sidelobe interference.

The analysis utilizes the knowledge of the slope of the plane of reflection. In the examples a zero slope was used. A nonzero slope could be easily accommodated by modifying Eqs. (10). However, the slope of the reflection plane is rarely known precisely. It can only be estimated. Any error in such an estimate translates into an error in the determination of the elevation angle. This is only a matter of complexity. The ratio of power received from the two pulses can be used instead of the symmetry condition to provide an additional equation. This, however, will work only if the target cross section is frequency independent in which case the power ratio is independent of target cross section. If the target is dispersive, its cross section varies from pulse to pulse and the additional equation introduces a new variable, namely, the unknown target cross section. Since a target cross section will usually depend on frequency, this presents a serious difficulty. To measure the slope of the reflection plane near the radar is as difficult as measuring the reflection coefficient and defeats the purpose of introducing the present method altogether.

An examination of Eq. (3) shows that changing the height of the antenna phase center is equivalent to changing the frequency as far as obtaining a phase change. Such a change does not affect the target cross section, and therefore offers a means to overcome the problem. However, the practicality of using height diversity in the context of complex monopulse is questionable. In the case of a dish antenna, it is impossible to realize this scheme easily. In the case of phased array, it could be accomplished by splitting the array and forming two or three independent monopulse beams. That is, by forming a sum and difference beam separately for each part of the array. It turns out that while this is a reasonable approach, there exists a simpler approach for phased arrays that does not require monopulse beams. This scheme is the Aperture Sampling method which will be described in Section III.

The normalized error signal can have a quadrature component due to an additional target present in the range cell or due to existing phase between the sum and difference channels. In order not to interpret this quadrature component as a result of multipath, one must have knowledge of the probability of having two targets in the range cell and of the phase response of the antenna in a wide angular range.

The method proposed here handles a single specular reflection. While in principle it could be extended to handle more than one specular reflection, provided one knows how many exist, such an extension is too complicated to be practical. It has no capability to compensate for diffuse reflection from the terrain. The presence of diffuse reflection causes an error which depends on the diffuse-to-specular reflection ratio.

The analysis neglected the variations in $\Gamma$, g, and E that take place from pulse to pulse. The sensitivity of this assumption can be determined by perturbation calculations in which the present solution is the zero-order solution.

The restrictions mentioned above contribute errors that may add to an unacceptable resultant error. The consequences of the need to know the slope of the effective reflection plane are considered to be the most serious difficulty with this scheme. Use of height diversity instead of frequency diversity as was suggested above does not offer a simple solution to this problem, hence the scheme is not judged to be an acceptable solution for a field radar.

C. Boresight Diversity

The most serious difficulty with the frequency-diversity version of Complex Monopulse is the fact that it requires knowledge of the slope of the plane of reflection. That is, without this information it becomes necessary to use the power ratio of two target returns as the fifth equation. This renders the scheme cross-section-dependent and therefore useful only in cases where the cross section does not vary substantially over the frequency band. In order to overcome this difficulty, an alternative scheme based on the Complex Monopulse was considered. This is the Boresight-diversity version.† The scheme is derived from the basic Complex Monopulse equation [Eq. (5)]:

$$\frac{1}{p}\,\frac{D}{S} = x + iy = \frac{A + uBe^{i\varphi}}{1 + ue^{i\varphi}} \quad , \qquad u = gr \quad . \tag{17}$$

One may easily show that as $g[S(B)/S(A)]$ varies while all the other parameters remain constant, Eq. (17) traces a circle in the complex plane. For various values of $\varphi$, a family of circles is obtained (see Fig. 11). These circles are orthogonal to the circles used in the frequency-diversity version. Let the unknown slope of the plane of reflection (a single specular reflection is assumed) be $E_s$. This parameter is incorporated in the analysis in order to demonstrate that indeed in this scheme one does not need to know it a priori. From Eq. (17), the explicit expressions for x and y, the real and imaginary parts of the normalized difference channel signal, are given by

$$x = \frac{A + Bu^2 + (A + B)\, u \cos\varphi}{1 + 2u\cos\varphi + u^2} \quad , \tag{18a}$$

$$y = \frac{(B - A)\, u \sin\varphi}{1 + 2u\cos\varphi + u^2} \quad . \tag{18b}$$

† The idea evolved in discussions that were held between Lincoln Laboratory and RCA.

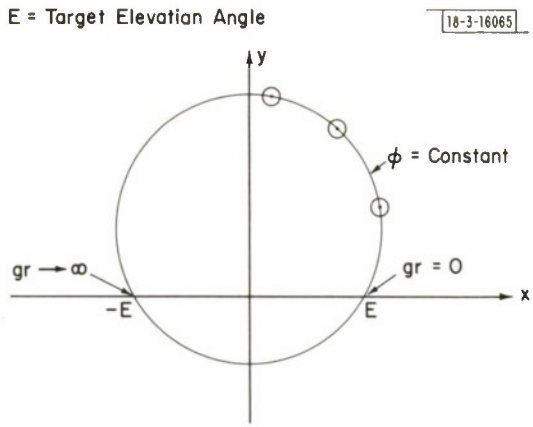


Fig. 11. Geometrical interpretation of the boresight diversity algorithm.

Elimination of u from these equations yields

$$(x^2 + y^2) \sin\varphi + y(B - A) \cos\varphi - x(B + A) \sin\varphi + AB \sin\varphi = 0 \quad . \tag{19}$$

Further trigonometric manipulations enable one to write (19) as follows:

$$(x - \frac{A + B}{2})^2 + (y + \frac{B - A}{2 \tan\varphi})^2 = \frac{(B - A)^2}{4 \sin^2\varphi} \quad . \tag{20}$$

From Eq. (20), the center and radius of the circle can be obtained; namely,

$$x_c = \frac{A + B}{2} \quad , \tag{21a}$$

$$y_c = -\frac{B - A}{2 \tan\varphi} \quad , \tag{21b}$$

$$R = \left| \frac{B - A}{2 \sin\varphi} \right| \quad . \tag{21c}$$

Eqs. (21b, c) show that whenever $\varphi = n\pi$, $n = 0, \pm 1 \ldots$, the circle degenerates into a straight line. It will be seen below that this poses a problem. The intersections of such a circle with the real axis are given by

$$x_i = x_c \pm \left| \sqrt{R^2 - y_c^2} \right| \quad . \tag{22}$$

This yields, after substituting Eqs. (21a-c),

$$x_1 = A = E - E_o \quad , \tag{23a}$$

$$x_2 = B = 2E_s - E - E_o \quad . \tag{23b}$$

Now, E, $E_o$, and $E_s$ are all referred to the radar coordinate system; that is, they are determined with respect to a coordinate system that is established independently of the local terrain. Therefore, the elevation angle can be determined from the upper intersection point ($x_1 > x_2$) without the need to know $E_s$, since $E_s$ does not affect the value of $x_1$ (Fig. 11).

For a given elevation angle, the phase between the direct and indirect return is fixed. By changing g, and provided that such a change does not change the phase, one can determine points on the corresponding circle. From three such points the circle's parameters can be determined.

Equation (22) can then be used to determine the upper intersection with the real axis which in turn yields the elevation angle via Eq. (23a).

A variation of g can be obtained in various ways. In the case of phased arrays, three monopulse beams can be formed simultaneously. They are squinted with respect to each other by a substantial fraction of a beamwidth so that each channel provides a point in the complex plane corresponding to a different value of g. An equivalent measurement can be obtained by using three successive pulses, each taken at a different beam-axis direction. Such an arrangement is particularly suited to a dish radar.

As was noted previously, there exists a difficulty in this scheme whenever the phase $\varphi$ is an integer multiple of $\pi$. In this case, the circle degenerates into a straight line and the algorithm becomes indeterminate. In an actual measurement, a solution is usually found because of measurement errors; however, it is characterized by extremely large angular errors. This effect can be seen in Fig. 12 which presents results of simulating random measurement errors.

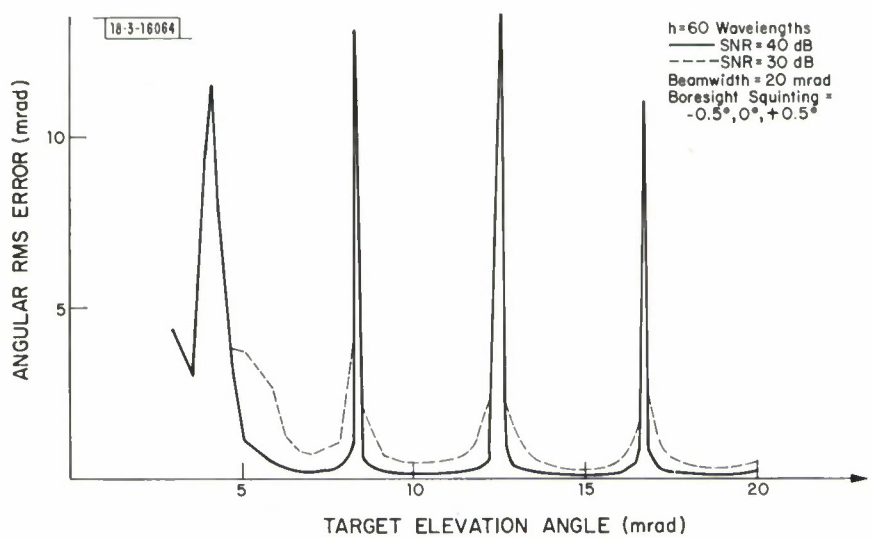


Fig. 12. Angular rms error for boresight diversity technique.

Large errors due to this effect are also observed at elevation angles that correspond to phase differences somewhat different from exactly an integer multiple of $\pi$. This clearly indicates a large sensitivity to measurement errors around the particular elevation angles that yield an integer multiple of $\pi$ phase. The width of the peaks is a function of signal-to-noise ratio, as indicated by the simulations that were performed for two values of SNR. The lower the phase center of the antenna, the larger is the separation between such peaks. It was felt that the method could be useful if there is a means to overcome the singular points (indeterminate set of equations). This could be achieved by frequency changes since $\varphi$ depends on frequency. In that case the elevation angle is estimated at three different frequencies, and the final estimate is the one corresponding to the average of the two closest measurements. An alternative approach is to use the fact that each elevation angle is characterized by a distinct set of complex voltages measured by the three monopulse beams. A similar approach is used extensively in the next section, and is called a minimizing search. The measured set of normalized complex

voltages $(v_1, v_2, v_3)$ is compared with a lookup table that includes sets $(v_1', v_2', v_3')$ of computed voltages for all possible combinations of amplitude, phase, and angle-of-arrival of two incoming plane waves in a given range. The set that minimizes the quantity $C = \sum_{i=1}^{3} |v_i - v_i'|^2$ is taken to be the estimate.

The question as to how to separate the three beams, or alternatively, what beam-axis pointing to choose is very crucial. From the point of view of accuracy, it can be seen intuitively that one would like to spread the three points on the circle as much as possible in order to reduce sensitivity to errors. (Such a situation was encountered in the frequency-diversity scheme.) This effect can be seen clearly in the simulation results. The simulations were performed with a fixed half-a-beamwidth squinting; that is, the beam axes were set at zero and ±1/2 a beamwidth elevation. It can be observed that at the lower elevation angles, the errors are larger and do not go down between singular points to the same level as in the case of higher elevation angles. This is explained by the fact that for lower elevation angles the angular separation between the target and its image is smaller, and for the same squint the obtained values of g are closer. That is, the three points on the circle are bunched together, and thus the algorithm is more sensitive to measurement errors. There are two factors that place an upper limit on the separation among the beams. If the beam is squinted more than half a beamwidth, the measurement is taken beyond the linear region of the difference pattern. In such a case, the theory developed here does not apply. The method could be extended to handle such cases by incorporating the exact nonlinear difference channel response. However, this represents a large increase in the degree of complication and it is not considered worthwhile. Another limitation on beam squinting is due to the possibility that for a large squint the target is viewed by at least two beams through a low pattern gain. This implies reduction in signal-to-noise ratio for the measurement of two points, which will cause larger errors. Therefore, a degradation of accuracy at extremely low elevation angles should be expected. This is a manifestation of the fact that at lower elevation angles, when the angular separation between the target and its image is smaller for a given SNR, the estimation error increases. Such a behavior was derived by Sklar and Schweppe[3] from general consideration.

An additional difficulty with the present scheme involves the question whether the phase between the direct and indirect return is the same for all three measurements. Such a condition is a necessary requirement, as the three points must belong to the same circle (Fig. 11). In the simulation, a flat surface was assumed, and the phase of the reflection coefficient was taken to be a constant, i.e., 180°. In the case of extremely rough terrain, the phase as well as the magnitude of the reflected wave will depend on the amount of squint. The specular reflection originates mostly in the first Fresnel zone. At low elevation angles, the Fresnel zone consists of an elongated ellipse. Contributions from small elements of this surface add vectorially, after being weighted by the antenna pattern. The phase and amplitude of the resultant reflected signal depend on the weighting. Since different beam pointings yield different weightings, the three points thus measured actually correspond to slightly different circles. This, of course, presents an additional source of error. This implies that for greater accuracy less squinting is desired.

## III. APERTURE SAMPLING

As was indicated in Section 1, the multipath problem in essence amounts to an angular resolution problem. When the elevation angle is within a beamwidth above the ground, the angular

separation between the target and its image may be less than a beamwidth. At the same time the range difference between them is smaller than the range resolution of the radar. Range resolution of the target from its image could be obtained in principle. However, such a capability requires extremely wide bandwidth or alternatively a very high antenna phase center. Both of these are not commonly available. For example, a 20-percent L-band radar has about 1 m range resolution, it could resolve in range the target and its image at 0.2° elevation, if its phase center were 143 m high. With the lack of range resolution it becomes necessary to resolve the target and its image in angle in order to measure the elevation angle of the target. In searching for a solution to this problem one is faced with the following questions.

(1) What is the angular resolving power of an antenna?

(2) What kind of angular precision is realizable when estimating simultaneously the angular parameters of two or more targets?

(3) What is the optimum processing? That is, how can one use the information available at the antenna aperture to obtain the best precision in a multiple plane-wave environment?

All three questions received a large amount of attention in the past and at present they are understood fairly well. The question of optimum processing is still an open question.

A. Principle and Limitations

It is a well established fact that the angular resolution of an antenna is about a beamwidth when the number of plane waves incident on it is not known a priori. This is a case when two targets have equal radar cross sections (RCS). The angular resolution deteriorates when there exists a difference in RCS. If, however, the number of incoming plane waves is known, then in the absence of noise the angular resolution is not limited.[4] Moreover, in the absence of noise it is possible to resolve plane waves no matter how close in angle-of-arrival they may be as long as their number does not exceed the number of half-wavelengths in the aperture. This is an ideal situation and represents a theoretical limit of performance. It also assumes that the phase of the incoming plane waves is not estimated. When, in addition, the phases of the incoming waves are estimated the number of plane waves that can be estimated is smaller. The aperture yields independent samples as long as they are taken $\lambda/2$ apart,† where $\lambda$ is the wavelength. Since the phase and amplitude of each such sample constitute independent data, an aperture of length L‡ yields $4L/\lambda$ independent measurements. These measurements can be used to uniquely solve for $4L/3\lambda$ incoming plane waves, since each plane wave is characterized by three unknown parameters, amplitude, phase, and angle-of-arrival. In most applications, one is interested in a smaller number of plane waves. In these cases fewer aperture samples, spaced more than $\lambda/2$, are sufficient. However, such a procedure narrows the unambiguous angular range and requires means to resolve the ambiguity. In a phased array, subarrays can be used for the sampling, and their directivity enables one to eliminate the ambiguity.

In the presence of noise, or other random measurement errors, the questions of resolution and precision cannot be separated. The angular resolving power certainly degrades. The question is how close in angle can two targets be before the errors in determining their angular

† This is the spatial equivalent of the temporal sampling theorem.

‡ The discussion is limited to a linear aperture for the sake of clarity.

position become larger than the error involved in measuring a single target. This question was addressed by Sklar and Schweppe[3] and Pollon and Lank[5] and others. Their work shows that the resolving power depends on the RF phase between the signals reflected from the two targets in addition to the signal-to-noise ratio. For SNR of 25 dB, resolution of between a half and a third of a beamwidth is possible. At 40 dB SNR, two targets may be resolved as close as 0.15 of a beamwidth. For multipath application, in the case of a flat surface and 25 dB SNR, this implies that acceptable measurements as low as 0.1° can be obtained by using a 0.5° beam. It should be realized that this is an upper bound on resolution that could be obtained if one would know how to use the aperture information in the optimal way. One might expect that larger errors or less resolution would be obtained in practice. The question of resolving more than two plane waves was investigated to a lesser extent. Assuming that the above resolution could be obtained when more than two plane waves are present, it is clear that for the case of 25 dB SNR the maximum realistic number to consider is three. More than three incoming plane waves that could be resolved would have to span an angular space wider than a beamwidth. In the case of multipath this is not a cause for concern since in most cases the additional distinct specular reflections span a large angular sector, in which case the theory indicates that they could be resolved.

B. Two Practical Methods

It is clear then that by utilizing independent samples of the received signal in the aperture, one should be able to obtain sufficient resolution for multipath compensation down to an elevation angle which is a small fraction of a beamwidth. Moreover, a scheme based on this approach could handle more than one specular reflection. The manner in which the aperture samples are processed to yield elevation angle estimates will now be described. Two processing algorithms are available at present. A closed-form solution that yields the parameters of the incoming plane waves was developed by Teledyne Micronetics.[6] An alternative approach using a minimizing search routine was developed by Hughes Aircraft Co.[7] In describing both algorithms it will be assumed that the number of incoming plane waves is known.

Let the amplitude, phase, and angle-of-arrival of the $j^{th}$ plane wave be denoted by $A_j$, $\varphi_j$, and $\alpha_j$. The voltage at the $n^{th}$ sampling element $V_n$ due to N plane waves is given by

$$V_n = \sum_{j=1}^{N} f(\alpha_j)\, A_j \exp(i\varphi_j) \exp(iknd \sin\alpha_j) \tag{24}$$

where $f(\alpha)$ is the voltage pattern of the sampling element, k is the free-space wave number, and d is the distance between the sampling elements. A linear uniformly spaced array is assumed here. An independent equation can be written for the complex conjugate of the element voltage

$$V_n^* = \sum_{j=1}^{N} f^*(\alpha_j)\, A_j \exp(-i\varphi_j) \exp(-iknd \sin\alpha_j) \quad . \tag{25}$$

Since coherent sampling is employed, $V_n^*$ is known independently. Denoting $\exp(iknd \sin\alpha_j)$ as $z_j$ and noting that $z_j^* = z_j^{-1}$, the sampled voltages can be expressed as

$$V_n = \sum_{j=1}^{N} B_j \exp(i\varphi_j)\, z_j^n \quad , \qquad n = 1, 2 \ldots M \tag{26a}$$

$$V_n^* = \sum_{j=1}^{N} B_j^* \exp(-i\varphi_j)\, z_j^{-n} \quad , \qquad n = 1, 2 \ldots M \tag{26b}$$

where $B_j = f(\alpha_j) A_j$. In all there are 2M equations, two for each of the M sampling elements. Elimination of $B_j e^{i\varphi_j}$ and its conjugate from Eqs. (26) yields the following set of linear equations

$$\begin{bmatrix} V_1, V_2 & \cdots & V_N \\ \cdot & & \cdot \\ \cdot & & \cdot \\ \cdot & & \cdot \\ V_{M-N} & \cdots & V_M - 1 \\ V_M^* & \cdots & V_{M-N+1}^* \\ \cdot & & \cdot \\ \cdot & & \cdot \\ \cdot & & \cdot \\ V_{N+1}^* & \cdots & V_2^* \end{bmatrix} \begin{bmatrix} a_N \\ \cdot \\ \cdot \\ \cdot \\ a_1 \end{bmatrix} = \begin{bmatrix} V_{N+1} \\ \cdot \\ \cdot \\ \cdot \\ V_M \\ V_{M-N}^* \\ \cdot \\ \cdot \\ \cdot \\ V_1^* \end{bmatrix} . \tag{27}$$

The unknowns are combinations of the $z_j$'s, namely,

$$a_n = (-1)^N \prod_{i=1}^{N} z_i \quad , \tag{28a}$$

$$a_\ell = (-1)^\ell \sum \quad \text{(products of } z_j \text{ taken } \ell \text{ at a time without repetition)}, \tag{28b}$$

$$a_1 = (-1) \sum_{i=1}^{N} z_i \quad . \tag{28c}$$

The unknowns $a_\ell$ are recognized to be the coefficients of a polynomial of degree N expressed in terms of its roots. Thus, the $z_j$'s are the roots of this polynomial. The first step in the algorithm is to solve the system of Eq. (27). This yields $a_\ell$'s. Once the $a_\ell$'s are known, the corresponding polynomial is solved for $z_j$. The angle-of-arrival is determined from $z_j$. To get the amplitude and phase, the values of $z_j$ are substituted in Eqs. (26), which then become a linear system that can be solved.

In the minimizing search† solution use is made of Eq. (24). The set of measurement voltages $(V_1, V_2, \ldots V_M)$ is compared to a set $(V_1', V_2', \ldots V_M')$ computed via Eq. (24) for an assumed amplitude, phase, and angle-of-arrival combination. The best approximation to the measured set is searched by varying in a systematic manner the parameters of the assumed incoming plane

† The author has used this solution to establish the performance of the Aperture Sampling technique. It is essentially the same as the one used by Hughes, but it is certainly not as efficient.

waves. The trial that provides the best approximation in the mean-square sense is taken to be the estimate. The best approximation is given by the set $(V'_1, V'_2, \ldots V'_M)$ that minimizes the quantity

$$C = \sum_{m=1}^{M} |V_n - V'_n|^2 \quad . \tag{29}$$

The choice of C was made here intuitively. The justification is the unique relation between the aperture illumination and the far field within the unambiguous angular range of the sampling elements array. The same criterion is obtained from general statistical arguments by forming a likelihood function and solving for the parameters that maximize that function.

In both approaches the number of incoming plane waves must be known. In practice this number must be estimated. When the search routine is used this can be simply accomplished by adding a dimension to the search. Starting with the largest number of plane waves that can be handled by the system (this depends on the number of sampling elements), the number of assumed plane waves is varied until the best estimate is obtained. In the closed-form solution approach the same procedure can be followed. In this case if the assumed number is larger than the actual number of plane waves, spurious estimates result. They can be distinguished by the fact that their amplitude is small and is usually close to the noise level. Upon detection of such spurious responses a solution with a reduced number of incoming waves is tried until all spurious signals are eliminated. In the case of multipath, for elevation angles below 1°, the reflected and direct returns have almost the same amplitude and both are substantially above the noise level. Additional specular reflections will be resolved only if they yield signals large compared to the noise level. Reflections of the same order of magnitude as the noise level could not be distinguished from spurious responses and would not be resolved. Such signals would not cause large error and would act like noise in limiting the precision of the system. For responses that are above the noise but small, the decision as to whether they are spurious responses or due to actual reflections should be handled statistically by setting a threshold that will correspond to a given probability of detection.

In subsequent sections the algorithms described here will be referred to as the Aperture Sampling technique.

C. Simulation Results

The Aperture Sampling method was evaluated by means of simulations. In Fig. 13, simulation results are presented for an aperture size of 75 wavelengths, corresponding to a 0.76° beamwidth. Three sampling elements 25 wavelengths apart and symmetrically located were used. The solid line presents the rms error as a function of true target elevation angle for the case where the reflection coefficient is −1, and only one specular reflection exists. It was obtained by means of the closed-form solution. It is seen that large errors occur in the vicinity of two angles. The large errors around these angles result from a singularity in the basic system of equations used in this algorithm. It can be seen by considering the specific system of equations. In the case of three sampling elements Eq. (27) reduces to:

$$\begin{bmatrix} V_1 & V_2 \\ V_3^* & V_2^* \end{bmatrix} \begin{bmatrix} a_2 \\ a_1 \end{bmatrix} = - \begin{bmatrix} V_3 \\ V_1^* \end{bmatrix} \quad . \tag{30}$$

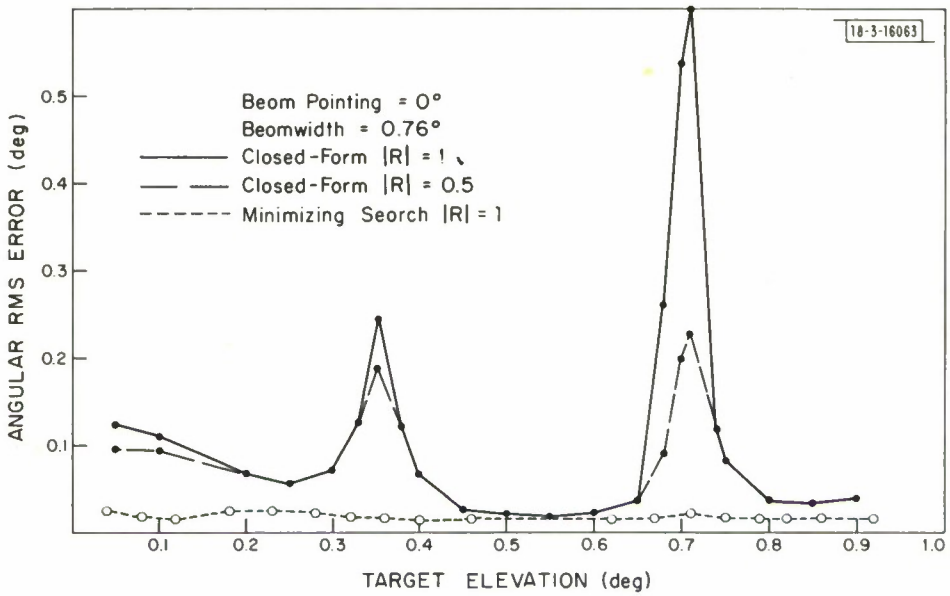


Fig. 13. Angular rms error for Aperture Sampling technique, SNR = 25 dB.

A singular condition occurs whenever the determinant of the matrix on the left-hand side vanishes. For target elevation angles below 1° and ground reflection coefficient of −1, one finds two angles (in addition to zero elevation) for which a singularity exists. One is an elevation of 0.712°, in which case $V_2 = 0$, the other is an elevation of 0.356° in which case the two equations are linearly dependent. This is in agreement with the simulations that show peak errors for these angles. Because of the presence of noise, the determinant does not vanish exactly, but is small. The errors are thus finite but large. For other elevation angles around these particular angles, the errors are also large. This indicates a sensitivity of the algorithm to perturbations in the vicinity of these angles. The dashed curve in Fig. 13 presents rms errors for the same setup in the case where the reflection coefficient was assumed to be −0.5. While under this condition, the singularity does not occur. It can be seen that substantial errors persist around the singular angles. This is due to the fact that the determinant is still small, and thus the algorithm is sensitive to the small perturbation caused by the noise.

It is noted that the singular conditions exist in the absence of noise. This seems to contradict the assertion made previously, in this section, that in the absence of noise there should not be any difficulty in resolving distinct plane waves no matter how close they are. Yet the algorithm is indeterminate for a few specific angles that correspond to a rather large angular separation. It turns out that in the absence of noise these singularities do not pose a problem. Since, then, the width of the peaks observed in Fig. 13 narrows to zero. Thus at any other angle the algorithm yields exact estimations with no errors. The singular condition can be detected by checking the value of the determinant. The exact angle can then be determined from the illumination along the aperture. For a given number of incoming plane waves within the unambiguous angular range, each such singularity is characterized by a distinct illumination that could be determined a priori. When the determinant vanishes, the corresponding measured aperture illumination is compared with the precomputed table of singular illuminations to yield uniquely the elevation angle.

The feature of being able to distinguish between the various singularities, which is so easily attained by the Aperture Sampling technique, can be extended and applied also when noise or other measurement errors are present. This is the basic idea behind the minimizing search approach. When noise is present, the peaks are broadened and the determinant does not vanish exactly. It is then required to perform a search to match the aperture illumination over a wider range of angles around the singular points. In that case an exact estimate could not be obtained; rather, a best estimate in the mean-square sense results [Eq. (29)]. The minimizing-search approach is to dispose with the closed-form solution and search the entire unambiguous angular range of the system.

The dotted curve in Fig. 13 presents simulation results obtained by using the minimizing-search routine. It was limited to the case of two incoming waves. The search was performed over the full unambiguous angular range. It is seen that indeed it does overcome the difficulties caused by the inherent singularities of the closed-form solution.

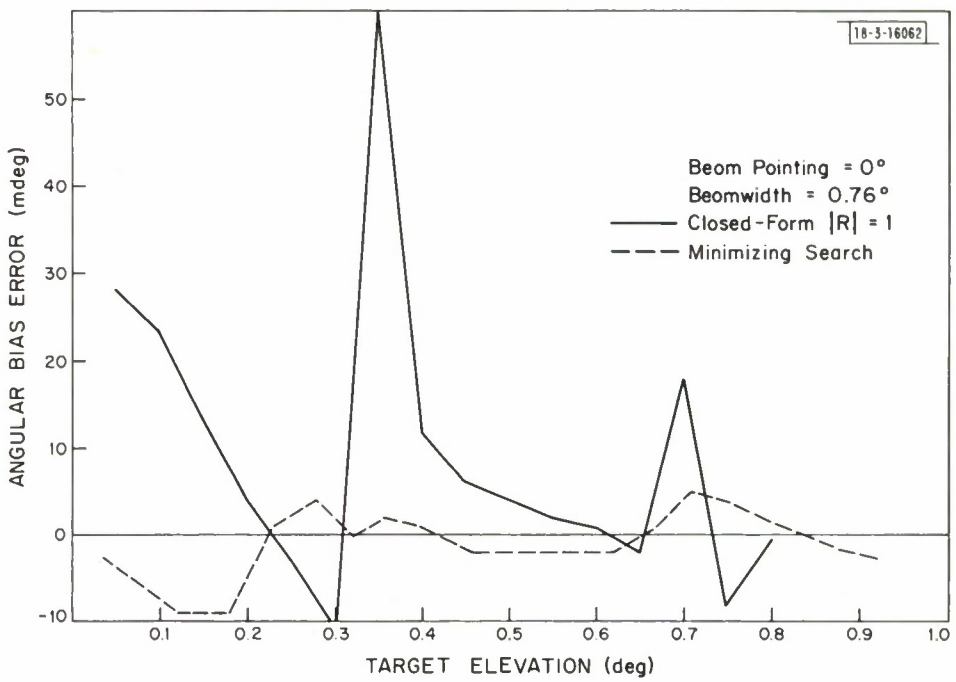


Fig. 14. Angular bias error for Aperture Sampling technique, SNR = 25 dB.

Figure 14 presents the bias (mean) errors found in the above simulations. The solid line presents the bias when the closed-form processing is used. It is seen that the bias is large around elevation angles that yield singularities. This is a serious problem and is unacceptable. The dashed line represents the bias obtained when the minimizing-search technique was used. It is seen that in general it is small. Below 0.2° a definite increase in bias is observed. While the bias is smaller than what could be obtained in a normal monopulse, it may not be small enough for certain applications. Since the errors are in part a function of the signal-to-noise ratio, this means that additional radar power will be required to meet more stringent specifications.

The performance of the aperture-sampling technique is comparable to the optimum angular precision that one could obtain in free space (without multipath). The optimum bound is given by[3]

$$\sigma = \frac{BW\sqrt{3}}{\pi\sqrt{2SNR}} \quad , \quad \sigma - \text{rms angular error.}$$

For the case simulated here, SNR = 25 dB and BW = 0.76°, the optimum bound is $\sigma$ = 0.017°. This bound implies a biasless estimate. However, the simulations yield a finite bias, and therefore a strict comparison to the theoretical bound is not possible. Observing that the bias for elevation angles above 0.25° is small (less than a quarter of the rms error) it seems plausible to combine the bias and rms errors and compare the sum to the optimum bound. This sum varies between 0.019° and 0.025°. This is clearly comparable to the theoretical value. An elevation of 0.25° represents an angular separation between the direct and indirect signals of 0.5° which is about 2/3 of a beamwidth. This too is in good agreement with Sklar and Schweppe[3] as far as resolution in the presence of noise is concerned. Their study shows that two components separated by at least 2/3 of a beamwidth could be resolved for such a SNR. For elevation angles below 0.25° an increase of bias as well as rms error is observed. The combined bias and rms error is about 0.034° which is about twice the theoretical bound. While this still may be considered as an acceptable performance it should be taken only in the context of resolving power. That is, such a performance could possibly be obtained if the terrain is indeed flat. In practice, this could hardly be the case. The Fresnel zone for an elevation angle of 0.25° extends as much as 16 km from the antenna (for the given case). For lower angles it extends even further. Under these circumstances earth curvature and existing mountain ranges must be included in the ground model (roughness can be neglected). The earth curvature reduces the magnitude of the reflection coefficient, and the possibility of a mountain range beyond a distance of 16 km limits how low an elevation angle one should consider. Therefore it is believed that the above simulations give an indication of only the resolving power below 0.25°. How meaningful they are in terms of a real terrain can be judged only with reference to a specific case. Finally, it ought to be emphasized here that the error magnitudes quoted above apply to the simulations only. In actual systems larger errors will be found due to the ever presence of errors other than random noise.

D. Multiple-Specular and Diffuse Ground Reflections

As was noted earlier the Aperture Sampling technique can be easily extended to handle more than just one specular reflection. Such an extension is rather involved, if possible at all, in the techniques described in the previous sections. The question then is how well does the Aperture Sampling technique perform in a multiple-specular environment. There are two situations of interest in this respect. One involves the presence of a few strong additional specular reflections, the other involves a number of reflections whose total energy is small compared to the principal specular reflection. Both cases are representative of a rough terrain. In the first case the additional specular reflections may be due to the existence of large obstructions. The second case describes a rough terrain without any outstanding distinct scatterers. A limited number of simulations were performed to evaluate the performance of the technique in these two cases. Rather than getting involved in a complicated terrain modeling that could be correlated to a specific terrain (a task that might be undertaken in future phases of the program), it was felt that some indication concerning the performance of the technique can be obtained from a simplified model of a rough terrain. In the case of strong multiple reflections one is concerned with

reflected signals which by themselves are larger than the noise level so that there exists for each, a high probability of detection, given the means to do so. The Aperture Sampling technique may have this capability. To test this case, large reflected signals with fixed angle-of-arrivals, amplitude, and phase were superimposed on the previously used flat ground model. In particular, two such components were used. The angle-of-arrival of these two components was chosen to simulate a reflected signal from a large obstacle within the first Fresnel zone. To accommodate two additional reflected signals, six sampling elements were used. Two typical cases of such simulations are given in Table I. The indicated signal-to-noise ratio in the table is the one that

TABLE I

MULTIPLE SPECULAR REFLECTIONS

| $E_T$ \ SNR | 55 dB | | 45 dB | | 35 dB | | 25 dB | |
|---|---|---|---|---|---|---|---|---|
| | Bias | rms | Bias | rms | Bias | rms | Bias | rms |
| 0.45 | 0.0 | 0.011 | −0.005 | 0.039 | −0.072 | 0.211 | 0.344 | 0.804 |
| −0.45 | 0.001 | 0.079 | −0.002 | 0.184 | 0.041 | 0.271 | 0.115 | 0.321 |
| −0.9 | −0.003 | 0.080 | 0.027 | 0.207 | 0.092 | 0.320 | 0.096 | 0.410 |
| −1.5 | 0.8 | 0.028 | −0.009 | 0.101 | 0.078 | 0.291 | 0.133 | 0.469 |
| | | | | | | | | |
| 0.55 | 0.002 | 0.067 | 0.002 | 0.026 | 0.038 | 0.120 | 0.036 | 0.182 |
| −0.55 | 0.395 | 0.397 | 0.418 | 0.348 | 0.483 | 0.350 | 0.442 | 0.385 |
| −0.9 | 0.105 | 0.338 | 0.226 | 0.386 | 0.258 | 0.492 | 0.426 | 0.445 |
| −1.5 | −0.442 | 0.447 | −0.594 | 0.542 | −0.223 | 0.678 | 0.104 | 0.738 |

$E_T$ – true target elevation

would be observed by the total aperture. The most obvious observation is that the ability to resolve multiple specular reflections depends on the SNR. It is seen that for a SNR of 25 dB, which is probably the one of primary interest, the performance is unacceptable. Comparing the two cases one may also conclude that the SNR is not the only factor that affects the performance in a multiple-specular environment. The second case, in which the elevation angle is 0.1° larger than the first case, shows that the performance is poor even for SNR of 55 dB. These simulations were performed using the closed-form processing. No attempt was made at this time to extend the search approach to handle more than one specular. The results shown here indicate that further work is needed in order to establish the performance of the Aperture Sampling technique in the presence of more than one specular reflection.

The presence of diffuse reflection was simulated by adding a few small reflections to the principal specular reflection. At the outset it was realized that, since the strength of each such component is of the same order of magnitude as the thermal noise, there is an extremely small probability of detecting and resolving each one individually. Therefore, accuracy of the estimate in the presence of such small components, when the system assumes the presence of only one specular reflection, was evaluated. Specifically, in one case, the specular reflection coefficient

was assumed −0.85 (rather than −1), and ten components were then superimposed on it. The ten components were chosen in magnitude to add to 0.15 if they turned out to be all in phase. In other words, the ratio of specular to the sum of the diffuse reflections is 15 dB. The phase of the individual components was assumed uniformly distributed between 0° and 360° and was selected randomly. Similarly, their angle-of-arrival was assumed uniformly distributed between 0° and −5°. Table 11 presents the results of these simulations. The first column describes the performance in the absence of multiple reflections. Comparison of these results to Fig. 13 shows small differences in the bias error. This is accounted for by the fact that here R = 0.85, and in this particular simulation computer time was traded for a coarser granularity in the search routine. In the rest of the table various combinations of multiple reflections were added to the specular reflection. The four cases shown in Table 11 include two diffuse-to-specular ratios, −10 dB and −15 dB, and the number of components used is 10 and 20. In all cases the SNR is 25 dB.

The results given in Table 11 provide some indication concerning the performance of the Aperture Sampling technique in the presence of diffuse reflection. An obvious conclusion is that the performance degrades as the ratio of diffuse-to-specular reflections increases. The effect is mainly an increase of the bias error, though a discernable simultaneous increase of rms error is observed for the case of −10 dB. The bias changes sign in an irregular manner as the elevation angle varies. This fact makes it difficult to suggest that some type of calibration could be used to eliminate it. It ought to be remembered that the processing assumed the presence of a single specular reflection. It seems that the variable bias represents an uncertainty across the range of elevation angles of interest here. It may be possible to specify bounds for this uncertainty as a function of the diffuse-to-specular ratio. In that case the radar processor could estimate the performance from an a priori estimate of this ratio. At any rate, one should realize that even the worst bias error in the presence of −10 dB diffuse reflection is 1/15 of a beamwidth. Such performance still surpasses the performance of a conventional monopulse in the presence of multipath.

The above evaluation should be qualified by observing that the rudimentary rough surface model represents a possible situation and not a specific terrain. It is based on the gross facts that diffuse reflection may have a random phase and arrives from a wide range of directions. It could not be related to the physical dimensions of the roughness or to the correlation length of such a surface. It is believed that it does represent a possible realization from an ensemble which is specified only by means of the diffuse-to-specular ratio.

The technique is being considered for application in a phased array. In this case it is postulated that the array is divided in the vertical direction (elevation) into three (or more) subarrays, each serving as a sampling element. In this approach the directivity in the transverse (azimuth) direction is maintained. The directivity of the sampling element in the vertical plane (elevation) depends on the number of sampling subarrays used. In the simulated case the total aperture beamwidth was 0.76°. Therefore, in the case of three elements, each has a beamwidth of about 2.28°. This was the motivation for limiting the range of angle-of-arrival of the diffuse components to 5° at most. It was felt that for larger angles the directivity of the subarray would reduce the strength of the arriving signals.

Based upon the simulations it is believed that the performance of the Aperture Sampling technique represents a substantial improvement over the schemes described in the previous section. This is clearly demonstrated when they are compared in the presence of a single specular

TABLE II

DIFFUSE REFLECTIONS

| E | Single Specular | | DS = −15 dB L = 10 | | DS = −15 dB L = 20 | | DS = −10 dB L = 10 | | DS = −10 dB L = 20 | |
|---|---|---|---|---|---|---|---|---|---|---|
| | Bias | rms | Bias | rms | Bias | rms | Bias | rms | Bias | rms |
| 0.11 | −0.016 | 0.017 | −0.008 | 0.019 | −0.011 | 0.016 | −0.002 | 0.023 | −0.008 | 0.018 |
| 0.16 | −0.002 | 0.024 | −0.008 | 0.028 | −0.013 | 0.027 | −0.007 | 0.021 | −0.010 | 0.021 |
| 0.21 | −0.004 | 0.025 | −0.006 | 0.023 | −0.006 | 0.023 | −0.009 | 0.014 | −0.008 | 0.015 |
| 0.26 | 0.006 | 0.017 | 0.019 | 0.016 | 0.019 | 0.016 | 0.024 | 0.016 | 0.024 | 0.016 |
| 0.31 | 0.004 | 0.019 | 0.020 | 0.025 | 0.019 | 0.025 | 0.037 | 0.018 | 0.001 | 0.021 |
| 0.36 | 0.004 | 0.014 | 0.026 | 0.016 | 0.024 | 0.016 | 0.038 | 0.013 | 0.034 | 0.010 |
| 0.41 | −0.004 | 0.013 | 0.015 | 0.020 | 0.015 | 0.020 | 0.028 | 0.024 | 0.029 | 0.007 |
| 0.46 | 0.008 | 0.010 | 0.028 | 0.014 | 0.027 | 0.014 | 0.040 | 0.014 | 0.040 | 0.013 |
| 0.51 | −0.008 | 0.012 | −0.013 | 0.013 | −0.007 | 0.013 | 0.035 | 0.018 | 0.040 | 0.018 |
| 0.56 | −0.002 | 0.015 | 0.013 | 0.014 | 0.014 | 0.013 | 0.023 | 0.014 | 0.025 | 0.015 |
| 0.61 | −0.004 | 0.019 | 0.018 | 0.016 | 0.017 | 0.017 | 0.036 | 0.019 | 0.039 | 0.019 |
| 0.66 | 0.002 | 0.018 | 0.007 | 0.017 | 0.008 | 0.016 | 0.021 | 0.021 | 0.020 | 0.020 |
| 0.71 | 0.005 | 0.020 | −0.006 | 0.021 | −0.003 | 0.021 | −0.010 | 0.025 | −0.011 | 0.022 |
| 0.76 | 0.006 | 0.014 | −0.002 | 0.017 | −0.003 | 0.017 | −0.011 | 0.012 | −0.014 | 0.018 |
| 0.81 | −0.005 | 0.015 | −0.021 | 0.015 | −0.021 | 0.016 | −0.027 | 0.014 | −0.029 | 0.014 |
| 0.86 | 0.011 | 0.011 | 0.005 | 0.015 | −0.004 | 0.015 | −0.009 | 0.014 | 0.007 | 0.016 |
| 0.91 | −0.012 | 0.015 | −0.020 | 0.011 | −0.020 | 0.012 | 0.023 | 0.013 | 0.023 | 0.013 |

E – true elevation

DS – diffuse-to-specular ratio

L – number of superimposed diffuse components

reflection. With regard to multiple-specular or diffuse reflections more work is needed. However, the simulations indicate that it may be possible to handle strong multiple reflections and to obtain acceptable performance in the presence of small diffuse reflection.

## IV. CONCLUSIONS

The comparative evaluation of the multipath compensation techniques presented in this report is based on their performance in the presence of a single specular reflection. It was felt that if a technique failed to show promise when tested under such circumstances, there was no point in subjecting it to a more complicated test which could include more specular components or diffuse reflections. The comparison indicates that the Aperture Sampling technique is definitely superior to other techniques provided the minimizing-search processing is used.

Experience has shown that in most cases, for a variety of terrains, at low elevation angles the ground effect consists of a single specular reflection, on which other small reflections are superimposed. Therefore, the failure of the Complex Monopulse techniques to offer a solution in the presence of a single specular reflection is enough to disqualify them as a viable solution to the problem. The simulations indicate that the Aperture Sampling technique performs well in the presence of a single specular reflection. In some cases, the ground effect includes additional strong specular reflections. In these cases one would like to be able to resolve the direct return in the presence of such strong specular reflections so that the target elevation angle could be estimated accurately. The Complex Monopulse techniques do not offer such an option. While in principle they may be extended to handle more than two plane waves, such an extension provcs to be extremely difficult and complicated and therefore not practical. The extension of the Aperture Sampling technique to handle more than two plane waves is simple. However, the limited number of simulations performed to assess its capability to resolve more than two plane waves did not yield definite positive conclusions. It is believed that more work in this area is needed. In particular, the minimizing-search routine should be extended to handle multiple strong reflections and studied before final conclusions are drawn.

The simple complex monopulse, comprising a displayed spiral or an equivalent analytical algorithm, suffers from inherent ambiguities. At present, no simple solution to this problem is in sight. In addition, seasonal and azimuthal variations in the terrain characteristics make it less realiable.

The frequency-diversity version of Complex Monopulse requires either the knowledge of the slope of the reflecting plane or the guarantee that the target's cross section is dispersionless. In the case of a rough terrain the knowledge of the effective slope of the reflection plane is as much a problem as the knowledge of the reflection coefficient. The assumption that the target cross section does not vary with frequency is not valid in most cases. It is therefore concluded that this technique could not be recommended as a means to overcome the multipath problem. The option to use height diversity implies the use of three monopulse channels with good linearity. This is far more complicated than the simple subdivision of the array as is suggested by the Aperture Sampling technique. Therefore, this approach is also rejected.

Similar problems plague the boresight-diversity version of the Complex Monopulse. The need, in the case of an array, for at least three monopulse channels with a wide linear range exists here too. The uneven illumination of the ground by the various beams induces angular errors. The large amount of squinting which is required for accurate estimates at low elevation angles results in high SNR degradation. In addition, no simple solution that could eliminate the

large errors encountered whenever the phase between the direct and indirect returns is an integer multiple of $\pi$ is available at present. Thus, this approach is judged unattractive.

In contrast to the Complex Monopulse techniques, the Aperture Sampling technique has been shown to yield accurate target elevation estimates in the presence of a single specular reflection without a priori knowledge of the terrain characteristics. The use of the minimizing-search processing eliminates the singular conditions encountered by the closed-form solution. The technique was also tested in the presence of diffuse reflections whose total power is as high as 10 dB below the specular reflection. Under these conditions, degradation in accuracy is observed. However, the resulting errors are small.

No definite conclusions concerning the ability of the Aperture Sampling technique to resolve more than two plane waves can be drawn at present. Based on the simulation results it is believed that this method is worth further analytical and experimental investigation. In particular, experiments to test its performance in the presence of a variety of physical terrains should be conducted.

In this report the signals were assumed to be narrowband. The effect of wide bandwidth on the performance of the Aperture Sampling technique should also be addressed in future studies. In particular, its interaction with the array's dispersive characteristics should be investigated. Its performance in estimating parameters other than elevation angle in the presence of multipath is also of interest.

## ACKNOWLEDGMENTS

The author would like to thank Mr. D. H. Temme for encouragement and helpful discussions, Dr. G. H. Knittel for critical review of the draft and helpful discussions, Mrs. Janet M. Reid and Miss Susan A. Rajunas for help in computer simulations.

## REFERENCES

1. S. M. Sherman, IEEE Trans. Aerospace Electron. Systems AES-4, 160-170 (1971).
2. D. K. Barton, H. R. Ward, Handbook of Radar Measurements (Prentice-Hall, Englewood Cliffs, N. J., 1969).
3. J. R. Sklar, F. C. Schweppe, "The Angular Resolution of Multiple Targets," Group Report 1964-2, Lincoln Laboratory, M.I.T. (14 January 1964), DDC AD-430185.
4. V. G. Welsby, J. Brit. IRE, 115-124 (1963).
5. G. E. Pollon, G. W. Lank, IEEE Trans. Aerospace Electron. Systems AES-4 (1968).
6. "Application Study of Wavefront Sampling Technique," RADC-TR-71-262, Teledyne Microwaves (November 1971).
7. J. E. Howard, "Application of Digital Parallel Processing (DIPPA) Techniques to Passive Direction Finding," AFAL-TR-73-263, Aerospace Group, Hughes Aircraft Company (June 1973).

## DOCUMENT CONTROL DATA – R&D

*(Security classification of title, body of abstract and indexing annotation must be entered when the overall report is classified)*

| | |
|---|---|
| 1. ORIGINATING ACTIVITY *(Corporate author)*<br>Lincoln Laboratory, M.I.T. | 2a. REPORT SECURITY CLASSIFICATION<br>Unclassified<br>2b. GROUP |
| 3. REPORT TITLE<br>Compensation of Multipath Angular Tracking Errors in Radar | |
| 4. DESCRIPTIVE NOTES *(Type of report and inclusive dates)*<br>Technical Report | |
| 5. AUTHOR(S) *(Last name, first name, initial)*<br>Kupiec, Israel | |
| 6. REPORT DATE<br>20 March 1974 | 7a. TOTAL NO. OF PAGES<br>36 / 7b. NO. OF REFS<br>7 |
| 8a. CONTRACT OR GRANT NO. F19628-73-C-0002<br>b. PROJECT NO. 7X263304D215<br>c.<br>d. | 9a. ORIGINATOR'S REPORT NUMBER(S)<br>Technical Report 501<br>9b. OTHER REPORT NO(S) *(Any other numbers that may be assigned this report)*<br>ESD-TR-74-138 |
| 10. AVAILABILITY/LIMITATION NOTICES<br>Approved for public release; distribution unlimited. | |
| 11. SUPPLEMENTARY NOTES<br>None | 12. SPONSORING MILITARY ACTIVITY<br>Office of the Chief of Research and Development<br>Department of the Army |

13. ABSTRACT

Multipath compensation techniques for radar applications are being evaluated. Three methods which comprise an extension of the conventional monopulse and a fourth that utilizes coherent samples taken across the antenna aperture were considered. The performance in the presence of a single specular reflection from the ground is compared by means of Monte Carlo computer simulations. The aperture sampling technique using a minimizing search processing is found to outperform the other methods.

14. KEY WORDS

Multipath compensation
Aperture sampling
Complex monopulse
Frequency diversity